

# Complexes of uranyl(II), vanadyl(II) and zirconyl(II) with orotic acid “vitamin B13”: Synthesis, spectroscopic, thermal studies and antibacterial activity

Moamen S. Refat \*

*Department of Chemistry, Faculty of Education, Suez-Canal University, Port Said, Egypt*

Received 31 August 2006; received in revised form 4 December 2006; accepted 4 December 2006

Available online 19 January 2007

## Abstract

A convenient method for the preparation of complexes of the uranyl  $[\text{UO}_2]^{2+}$ , vanadyl  $[\text{VO}]^{2+}$  and zirconyl  $[\text{ZrO}]^{2+}$  ions with vitamin B13 (Orotic acid;  $\text{H}_3\text{OA}$ ) is reported and this has enabled three complexes of orotate anion ( $1^-$ ) to be formulated:  $[\text{M}(\text{C}_5\text{H}_3\text{N}_2\text{O}_4)_2(\text{H}_2\text{O})_2] \cdot (\text{H}_2\text{O})_n$  [where  $\text{M} = [\text{UO}_2]^{2+}$ ,  $[\text{VO}]^{2+}$ ,  $[\text{ZrO}]^{2+}$ ;  $n = 1, 6, 3$ , respectively]. The new bisorotate  $(\text{H}_2\text{OA})^{1-}$  complexes were synthesized and characterized by elemental analysis, molar conductivity, spectral methods (UV–vis, mass,  $^1\text{H}$  NMR and mid infrared spectra), and simultaneous thermal analysis (TG and DTG) techniques. Physical measurements indicate that the neutral orotic acid ligand in its mono/anion form, is bonded to oxometal ions through the carboxylic groups (two monodentate orotate anions and complete the coordination sphere by coordinated water molecules). The molar conductance data confirm that the orotate complexes are non-electrolytes. The X-ray powder diffraction (XRD) as well as scanning electron microscopy (SEM) shows that the studied complexes have amorphous structures. The kinetic thermodynamic parameters, such as,  $E^*$ ,  $\Delta H^*$ ,  $\Delta S^*$  and  $\Delta G^*$  are calculated from the DTG curves. The antibacterial activity of the orotic acid and their complexes was evaluated against gram positive/negative bacteria.

© 2006 Elsevier B.V. All rights reserved.

*Keywords:* Vitamin B13; Infrared spectra; Antibacterial activity; Thermal analysis; Kinetic parameter

## 1. Introduction

Orotic acid (OA), also known as vitamin B13, is a precursor of nucleic acid bases acting as an intermediate in pyrimidine synthesis, particularly the uracil base [1]. It was found in cells and body fluids of many living organisms. This compound is applied in medicine as bio-stimulator of the ionic exchange processes. There is a great interest in the orotic acid relation to food protection and nourishment research. A reliable assignment of its vibrational spectra [2] is a useful basis in the study of the interaction with other chemical species present in the biological milieu. From this point of view there are problems with the solubility in water of this molecular compound. Inclusion

complexes in cyclodextrins could be a possibility due to the water solubility increase of these supramolecular compounds. The perfect compatibility of these inclusion complexes with the living organisms must be taken into account by their frequent use now as antiinflammatory [3,4], cardiovascular [5], antidepressive or ophthalmologic drugs [6].

Orotic acid (6-carboxy uracil, 1,2,3,6-tetrahydro-2,6-dioxo-4-pyrimidine carboxylic acid,  $\text{H}_3\text{OA}$ ) (Fig. 1) is closely related to the biologically important pyrimidine bases [7,8]. Besides its biological importance, orotic acid and its substituted derivatives which may be viewed as substituted uracils are also interesting ligands. Since they are potentially multidentate, the coordination may occur through the heterocyclic nitrogens of the pyrimidine ring, the exocyclic carbonyl oxygens, and the carboxylic group. However, studies on its coordination properties in solution

\* Tel: +20127649416.

E-mail address: [msrefat@yahoo.com](mailto:msrefat@yahoo.com)

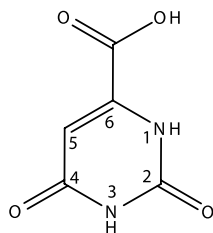


Fig. 1. Numbering Scheme of orotic acid ( $H_3OA$ ).

and in the solid state show that orotic acid coordinates mainly via N(1) and the carboxylate group. The only exceptions known thus far are the copper(II) complex of 5-nitroorotic acid, which coordinates via the N(1) and N(3) nitrogens [9]. While one of the roles of the magnesium ion is to change orotic acid to an N(1) deprotonated dianion, orotic acid does not enter the inner coordination sphere of the metal in magnesium bisorotate (1–,  $H_2OA$ ) octahydrate [10] and in zinc bisorotate octahydrate [11]. However, the complexity of the pyrimidine system results also from pH changes. Between pH 3 and 9, orotic acid is present in aqueous solutions mainly as the orotate anion (the carboxylic group has  $pK = 2.07$ ). N(3)–H in which the N(1) atom is unsubstituted, is obtained by abstraction of a second proton ( $pK = 9.45$ ) and, according to previous observations on related uracil anion systems, should be present together with the N(1)–H tautomer [12,13]. UV light absorption studies, potentiometry and linear free energy relationships for proton dissociation [14] have been used to investigate the complexation of zinc(II), cobalt(II), manganese(II), cadmium(II), copper(II) and nickel(II) with orotic acid in solution. It was concluded that, in neutral or slightly acidic pH, the ions of Zn(II), Co(II), Mn(II) and Cd(II) coordinate through the carboxylate group while Cu(II) and Ni(II) through the carboxylate and adjacent N(1). Spectroscopic investigation of the interaction of nickel(II) with orotic acid [15] revealed binding of the metal to the carboxylate and, in some cases, to the adjacent N(1) and the O(4) sites. The crystal structures of the Ni(II) [16,17], Mg(II) [18], Co(II) [19], Zn(II) [20] orotate complexes have been described where orotate dianions act as bidentate ligand.

Relatively little information is available regarding the compounds with orotate monoanion ( $H_2OA$ , 1–). Due to the high reactivity and different coordination modes of orotic acid towards metal ions, this paper, describes the first structurally characterized solid complexes of neutral orotic acid with uranyl(II), vanadyl(II) and zirconyl(II) ions. The great importance of vanadyl that is work like insulin in the body to increase the amount of glucose and amino acids driven into the muscles, and zirconyl is a brominated zirconium oxide. The investigation of these prepared complexes was carried out using elemental analysis CHN, molar conductivity, (infrared, electronic UV–vis,  $^1H$  NMR and mass spectra), X-ray diffraction analysis, scanning electron microscope, TG and DTG techniques as well as kinetic parameters.

## 2. Experimental

### 2.1. Materials and instrumentation

All chemicals were reagent grade and were used without further purification. Orotic acid was purchased from Aldrich Chemical Co.,  $UO_2(NO_3)_2 \cdot 6H_2O$  (Fluka Co.),  $VOSO_4 \cdot xH_2O$  and  $ZrOCl_2 \cdot xH_2O$  from (Aldrich Co).

Carbon and hydrogen contents were determined using a Perkin-Elmer CHN 2400 in the Micro-analytical Unit at the Faculty of Science, Cairo University, Egypt. The metal content was found gravimetrically by converting the compounds into their corresponding oxides.

IR spectra were recorded on Bruker FT-IR Spectrophotometer ( $4000\text{--}400\text{ cm}^{-1}$ ) in KBr pellets. The UV–vis, Spectra were obtained for the DMF solution ( $10^{-3}\text{ M}$ ) of the orotic acid and their three complexes with a Jenway 6405 Spectrophotometer using 1 cm quartz cell, in the range 500–200 nm. Molar conductivities of freshly prepared  $1.0 \times 10^{-3}\text{ mol/dm}^3$  DMF solutions were measured using Jenway 4010 conductivity meter. Mass spectra of the orotate (1–) complexes were checked using AEI MS 30 mass spectrometer at 70 eV.  $^1H$  NMR spectrum of  $[UO_2]^{2+}$  complex was recorded on Varian Gemini 200 MHz spectrometer using  $DMSO-d_6$  as solvent and TMS as an internal reference. Thermogravimetric analysis (TGA and DTG) were carried out in dynamic nitrogen atmosphere (30 ml/min) with a heating rate of  $10\text{ }^\circ\text{C/min}$  using a Shimadzu TGA-50H thermal analyzer. The X-ray diffraction patterns (XRD) were obtained on a Rigaku diffractometer using  $Cu/K\alpha$  radiation. Scanning electron microscopy (SEM) images were taken in JEOL-840 equipment, with an accelerating voltage of 15 KV.

### 2.2. Preparations

Initial experiments were performed in order to find, if possible, a general method for the preparation of orotic acid complexes. But because of the low solubility of orotic acid in water and also the difficulty in controlling the extent of ionization in alkaline medium, the reaction of orotic acid with lithium hydroxide in water at room temperature; subsequent addition of aqueous metal salt solutions did not appear to lead to complex formation. However, it was found that by heating the  $H_3OA\text{--}LiOH \cdot H_2O$  solution to  $70\text{ }^\circ\text{C}$  for 30 min, followed by addition of the metal salts, complexes formed readily (this method not carried out previously).

A general method is: orotic acid (1.56 gm, 0.01 mol) and  $LiOH \cdot H_2O$  (0.42 gm, 0.01 mol) were dissolved in water (40 ml) and the solution heated to  $70\text{ }^\circ\text{C}$  for 30 min. The metal salts were dissolved in a minimum quantity of water and the solutions mixed with vigorous stirring (for (1:2); (metal:ligand) ratio). Precipitations were almost instantaneous, but stirring was continued for 15 min. The complexes were filtered, washed with water (20 ml hot water), alcohol (15 ml), and dried *in vacuo* over  $CaCl_2$ . It was

found that lithium hydroxide powder was preferable to sodium or potassium hydroxides pellets as more accurate weighting is possible with powder. The yields were found around 70% based on the metal salts. The compounds resulted have low solubility in water and in common organic solvents, except the  $[\text{UO}_2]^{2+}$  compound has slightly partially dissolves upon gentle heating in DMSO.

### 2.3. Antibacterial investigation

For these investigations the filter paper disc method was applied. The investigated isolates of bacteria were seeded in tubes with nutrient broth (NB). The seeded NB ( $1 \text{ cm}^3$ ) was homogenized in the tubes with  $9 \text{ cm}^3$  of melted ( $45^\circ \text{C}$ ) nutrient agar (NA). The homogeneous suspensions were poured into Petri dishes. The discs of filter paper (diameter 5 mm) were ranged on the cool medium. After cooling on the formed solid medium,  $2 \times 10^{-5} \text{ dm}^3$  of the investigated compounds were applied using a micropipette. After incubation for 24 h in a thermostat at  $25\text{--}27^\circ \text{C}$ , the inhibition (sterile) zone diameters (including disc) were measured and expressed mm. An inhibition zone diameter over 8 mm indicates that the tested compound is active against the bacteria under investigation.

The antibacterial activities of the investigated compounds were tested against *Escherichia Coli* and *Salmonella* (Gram negative bacteria) and *Bacillus subtilis* and *Staphylococcus aureus* (Gram positive bacteria). In the same time with the antibacterial investigations of the  $[\text{UO}_2]^{2+}$ ,  $[\text{VO}]^{2+}$ , and  $[\text{ZrO}]^{2+}$  complexes, the ligand was also tested, as well as the pure solvent. The concentration of each solution was  $5 \times 10^{-3} \text{ mol dm}^{-3}$ . Commercial DMF was employed to dissolve the tested samples.

### 3. Results and discussion

The results of the elemental analysis and some physical characteristics of the obtained compounds are given in Table 1. The complexes were synthesized using a 1:2 (metal:ligand) mole ratio of all reactants. The elemental analysis (Table 1) of the complexes indicates a 1:2 metal to ligand stoichiometry, too. The complexes are air-stable, hygroscopic, with high melting points, insoluble in  $\text{H}_2\text{O}$ , but partly soluble in dimethylformamide, DMF. The molar conductivities of  $10^{-3} \text{ mol dm}^{-3}$  solutions of the complexes in DMF (Table 1) indicate that the complexes as non-electrolytes in DMF.

It is worth mentioning that most studies of orotic acid complexes in the solid phase have found that orotic acid is in the dianion form [16,20–23]. It is, therefore, of great interest to examine the coordination behavior of orotic acid at neutral pH values with using (LiOH). Attempts to crystallize the products in DMF have failed so that, in this study used many techniques of analysis to prove the structure of the synthesized complexes.

#### 3.1. Infrared spectra

The infrared spectra of orotic acid and their complexes have received little attention [24,25]. In publications where the spectrum appears minor assignments are attributed in comparison with similar compounds [26–28]. By contrast, the spectra of uracil and its derivatives have been studied by quantum mechanical methods. Tentative assignments of IR bands of  $[\text{UO}_2]^{2+}$ ,  $[\text{VO}]^{2+}$  and  $[\text{ZrO}]^{2+}$  complexes are present in Table 2, and Fig. 2. The assignments of the studied complexes have been comparing with the spectra of  $\text{H}_3\text{OA}$  and  $\text{NaH}_2\text{OA}$  (1–) [24].

The IR spectra of the  $[\text{UO}_2]^{2+}$ ,  $[\text{VO}]^{2+}$  and  $[\text{ZrO}]^{2+}$  complexes exhibited characteristic features (donation sites) in the  $-\text{OH}$  (acid), ketone ( $\text{C}(2)=\text{O}$  and  $\text{C}(4)=\text{O}$ , carboxylate and  $\text{NH}$  ( $\text{N}(1)-\text{H}$  and  $\text{N}(3)-\text{H}$ ) regions. The spectrum of the  $[\text{VO}]^{2+}$  complex has slightly different from  $[\text{UO}_2]^{2+}$  and  $[\text{ZrO}]^{2+}$  complexes (in the region of crystallized water) due to the presence of number of lattice water leading to different hydrogen bonding interactions with the coordination water and orotate anions.

- (i) In the  $\nu(\text{O}-\text{H})_{\text{water}}$  region the spectra of the three mentioned complexes show one strong broad band in the range of  $3420\text{--}3480 \text{ cm}^{-1}$  attributed to the presence of coordination water [29]. Coordination and crystal water stretching modes appear between  $3600\text{--}3420 \text{ cm}^{-1}$  with the crystal water appearing at frequencies higher than these of coordination product.
- (ii) Deprotonation of  $\text{N}(1)$  results in disappearance of the bands at *Ca.*  $3200$  and  $1430 \text{ cm}^{-1}$  attributed to the stretching and bending  $\text{N}(1)-\text{H}$  vibrations. This is noted in cases where the orotate bind through the  $\text{N}(1)$  atom. The crystal structure of the  $[\text{Ni}(\text{HOA})(\text{H}_2\text{O})_4]\cdot\text{H}_2\text{O}$  [16] and  $[\text{Cu}(\text{HOA})(\text{NH}_3)_2]$  [21] complexes showed bidentate binding of orotic acid through  $\text{N}(1)$  and the carboxylate group. No such

Table 1  
Analytical and physical data of the investigated compounds

Complexes	M.Wt	Yield (%)	Color	M.P ( $^\circ\text{C}$ )	Anal. (%) found (Calcd.)			$A$ ( $\Omega^{-1} \text{ cm}^2 \text{ mol}$ )
					C	H	N	
$[\text{UO}_2(\text{C}_5\text{H}_3\text{N}_2\text{O}_4)_2(\text{H}_2\text{O})_2]\cdot(\text{H}_2\text{O})$	634	73	Yellow	>300	18.90 (18.90)	2.05 (1.89)	8.67 (8.83)	2.76
$[\text{VO}(\text{C}_5\text{H}_3\text{N}_2\text{O}_4)_2(\text{H}_2\text{O})_2]\cdot 6(\text{H}_2\text{O})$	521	69	Green	>300	22.70 (23.00)	3.98 (4.22)	10.54 (10.70)	6.70
$[\text{ZrO}(\text{C}_5\text{H}_3\text{N}_2\text{O}_4)_2(\text{H}_2\text{O})_2]\cdot 3(\text{H}_2\text{O})$	507	71	White	>300	23.50 (23.70)	2.96 (3.16)	10.85 (11.00)	4.51

Table 2  
IR frequencies ( $\text{cm}^{-1}$ ) of orotic acid ( $\text{H}_3\text{OA}$ ), sodium orotate ( $\text{NaH}_2\text{OA}$ ), uranyl, vanadyl and zirconyl complexes

$\text{H}_3\text{OA}$	$\text{NaH}_2\text{OA}$	$[\text{UO}_2]^{2+}$	$[\text{VO}]^{2+}$	$[\text{ZrO}]^{2+}$	Assignments
–	3500 w, sh	3570 sh	3589 w 3567 w	3505 sh	$\nu(\text{OH})$ ; Cyst water
–	–	3447 s,br	3476 s,br	3421 s,br	$\nu(\text{OH})$ ; Coord. water
3155 sh	3200 s	3212 s	3218 s	3213 s	$\nu(\text{N1-H})$
3099 m	3100 s	3114 w	3117 w	3114 w	$\nu(\text{C5-H})$
3020 vw	2950 s,br	2971 s,br	2989 s,br	2972 br	$\nu(\text{N3-H})$
3002 w	2900 sh	2800 s	2812 s	2800 s	
2950 sh					
2810 s					
2560 w	–	–	–	–	$\nu(\text{OH})$ acid
2490 s,br					Hydrogen bond
1703 vs	1740 s	1735 vs	1738 vs	1734 vs	$\nu(\text{C=O})$ acid + $\nu(\text{C2=O})$
1650 vs	1710 sh	1692 vs	1685 vs	1688 vs	$\nu(\text{C4=O}) + \nu(\text{C=C})$
	1690 s				
1518 s	1625 sh	1653 sh	1653 sh	1654 sh	$\nu_{\text{asym}}(\text{COO}^-) + \text{ring vib.} + \delta(\text{H}_2\text{O})$
	1493 m	1625sh	1561 w	1495 s	
		1494 s	1497 s		
1435 vs	1425 s	1426 s	1429 s	1426 s	$\delta(\text{N1-H}) + \text{ring vib.}$
1405 s					
1327 s	1385 s	1383 vs	1389 vs	1384 vs	$\nu_{\text{sym}}(\text{COO}^-)$
1263 vs	1290 m	1300 w,sh	1300 w,sh	1300 w,sh	$\nu(\text{C6-C7}) + \nu(\text{C-C}) + \nu(\text{C-N})$
	1270 sh	1232 s	1233 m	1232 s	
	1233 m		1182 w		
1126 m	1105 w	1106 vw	1113 s	1106 w	CH wagging + ring dif. + ring vib. $\nu(\text{M=O})$ [M = V and Zr]
1010 s	1015 m	1039 vw	1041 w	1039 vw	
982 s	960 w	1017 s	1017 m	1017 s	
			960 vw		
928 s	925 s	927 vs	931 s	928 s	$\delta(\text{N-H}) + \text{ring vib.} + \nu(\text{U=O})$
888 vw	880 sh	854 s	855 s	855 s	$\nu(\text{C-H}) + \nu(\text{C-C}) + \text{out-of-plane } \delta_r(\text{H}_2\text{O})$
860 s	845 s	792 w	798 vw	793 sh	
832 vw	790 s	778 s	780 s	778 vs	
729 vs	775 s	759 vw		759 sh	
	755 s				
	725 w				
649 w	630 m	637 s	640 s	671 vw	$\text{C2=O} + \text{C4=O bending} + \delta(\text{ring})$ ring def.
601 s	595 w	598 s	598 s	637 s	
551 vs	553 s	553 vs	552 vs	599 s	
460 s	508 m	508 s	510 m	553 vs	
437 vw	428 s	433 vs	439 s	509 s	
				432 vs	

br, broad; m, medium; s, strong; sh, shoulder; w, weak;  $\nu$ , stretching;  $\delta$ , bending.

assignment (the stretching and bending bands of  $\text{N}(1)\text{-H}$ ) was possible in this study, that these assignments,  $\nu(\text{N}(1)\text{-H}) + \delta(\text{N}(1)\text{-H})$ , are present in the  $[\text{UO}_2]^{2+}$ ,  $[\text{VO}]^{2+}$  and  $[\text{ZrO}]^{2+}$  complexes (Table 2) confirming the interaction not through  $\text{N}(1)\text{-H}$  but coordination mode is a monodentate.

- (iii) The carbonyl groups ( $\text{C}(2)\text{=O}$  and  $\text{C}(4)\text{=O}$ ) of the ring appear as two main peaks at 1700 and  $1650 \text{ cm}^{-1}$  in the free acid, the comparison between the infrared spectra of the free acid and its sodium salt, whose characterized [24], a shift is observed for the 1700 and  $1330 \text{ cm}^{-1}$  bands, corresponding to the asymmetric and symmetric stretching of the carboxylate group which appear at 1625 and  $1385 \text{ cm}^{-1}$  in sodium salt. These shifts are expected, when going from the acid to the salt. Similar shifts are observed in the complexes prepared ( $[\text{UO}_2]^{2+}$ ,  $[\text{VO}]^{2+}$  and  $[\text{ZrO}]^{2+}$  complexes), indicating an

interaction between the metal salt and the carboxylate group that ranges from the covalent to ionic depending on the shifts of the two bands. It was found that orotic acid interacts with all of these metal ions in the anionic form and coordinates in a monodentate feature through its carboxylate group to  $[\text{UO}_2]^{2+}$ ,  $[\text{VO}]^{2+}$  and  $[\text{ZrO}]^{2+}$  ions. This result is in accord with the n.m.r. data of  $[\text{UO}_2]^{2+}$  complex, that also indicate coordination of metal to the carboxylate group (monodentate).

- (iv) Another important band in distinguish between mono and bidentate coordination of orotate ligand ( $\text{H}_3\text{OA}$ ) is the stretching  $\nu(\text{C}(6)\text{-C}(7))$  band that in case of  $\text{NaH}_2\text{OA}$  appears with medium intensity at of  $1290 \text{ cm}^{-1}$ . This band shifted to higher frequencies ( $48$  and  $35 \text{ cm}^{-1}$ ) in the complexes of orotate ( $2\text{-}$ ) ligand, it is found in the cases where the metal ion coordinates through the carboxylate group and the

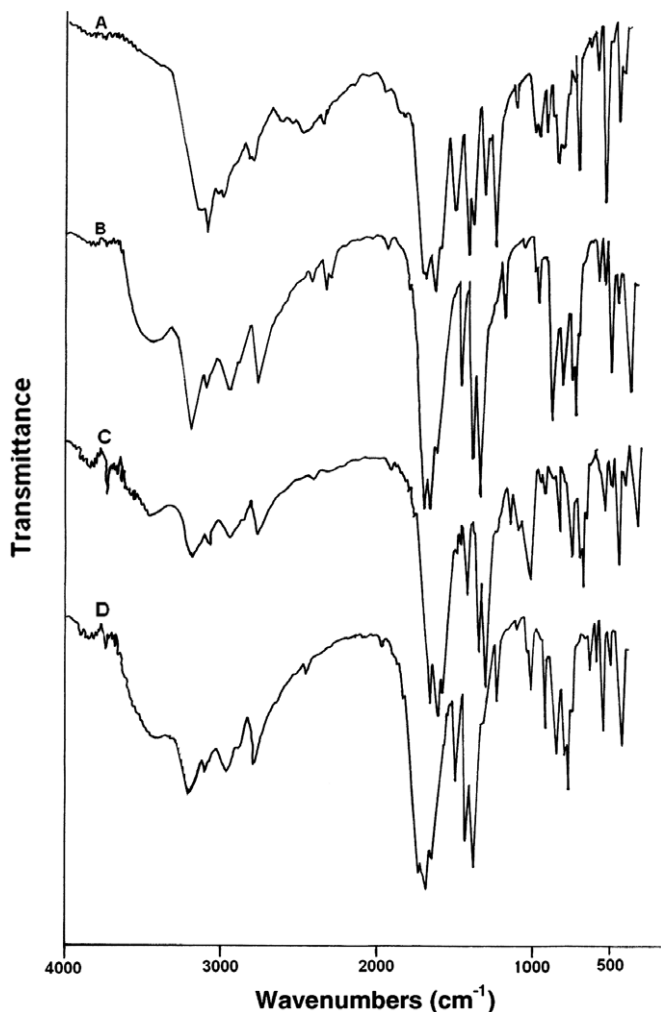


Fig. 2. Infrared spectra of: (A), orotic acid; (B), uranyl(II); (C), vanadyl(II); and (D), zirconyl(II) compounds.

N(1) [16,21]. While monodentate [24] of the metal through the carboxylate group results in smaller up field shift (+2 to +15  $\text{cm}^{-1}$ ). For the  $[\text{UO}_2]^{2+}$ ,  $[\text{VO}]^{2+}$  and  $[\text{ZrO}]^{2+}$  orotate complexes, this shift to 10  $\text{cm}^{-1}$  (because it present in 1300  $\text{cm}^{-1}$  with weak shoulder intensity) denoting coordination with the carboxylate group as monodentate.

- (v) The strong broad band around 2500  $\text{cm}^{-1}$ , which assigned to  $\nu(\text{OH})$  acid is absent in the all complexes resulted, this attributed to the involvement of carboxylic group of the free acid in the complexation.
- (vi) For the monodentate carboxylate coordination to the metal ion, observed in the structure of all prepared complexes, the relationship  $\Delta_{\text{Complex}} > \Delta_{\text{sod. orotate}}$  to apply [30], where  $\Delta = \nu_{\text{asym}}(\text{COO}) - \nu_{\text{sym}}(\text{COO})$ . [ $\Delta_{\text{sod. orotate}} = 240 \text{ cm}^{-1}$ ;  $\text{UO}_2(\text{II}) = 242 \text{ cm}^{-1}$ ;  $[\text{VO}]^{2+} = 264 \text{ cm}^{-1}$  and  $[\text{ZrO}]^{2+} = 270 \text{ cm}^{-1}$ ].
- (vii) The infrared spectra of all three complexes exhibit bands refer to  $\nu_{\text{asym}}$  and  $\nu_{\text{sym}}(\text{O-H})$  and  $\delta(\text{H}_2\text{O})$  vibration in the regions above 3400  $\text{cm}^{-1}$  and weak shoulder band around 1620  $\text{cm}^{-1}$ , respectively, this

meaning the presence of water molecules perhaps outside or inside coordination sphere of the complexes, also the presence of strong band at 855  $\text{cm}^{-1}$  in all complexes attributed to the rocking vibration motion,  $\delta_r(\text{H}_2\text{O})$ , of coordination water molecules, this confirm that  $\text{H}_2\text{O}$  molecules in the complexes are inside the coordination sphere. This notification was also supported by thermal analysis.

- (viii) The  $\nu(\text{U=O})$  vibration in the uranyl complex is observed as expected as a very strong band at 927  $\text{cm}^{-1}$  is a good agreement with those known for many dioxouranium(VI) complexes [31,32]. On the other hand concerning, the infrared spectra of  $[\text{ZrO}]^{2+}$  and  $[\text{VO}]^{2+}$  complexes show a strong and medium absorption band at 1017  $\text{cm}^{-1}$  due to  $\nu(\text{V=O})$  and  $\nu(\text{Zr=O})$  as expected [33].

### 3.2. Molar conductance measurements

The molar conductivity values for the orotate complexes in DMF solvent ( $10^{-3} \text{ mol dm}^{-3}$ ) were in the range of (2–7)  $\Omega^{-1} \text{ cm}^2 \text{ mol}^{-1}$ , suggesting them to be non-electrolytes (Table 1). Conductivity measurements have frequently been used in structural of metal chelates (mode of coordination) within the limits of their solubility. They provide a method of testing the degree of ionization of the complexes, the molar ions that a complex liberates in solution (in case of presence anions outside the coordination sphere), the higher will be its molar conductivity and vice versa. It is clear from the conductivity data that the complexes present seem to be non-electrolytes. Also the molar conductance values indicate that the anions may be present inside the coordination sphere or absent. This results were confirmed from the chemical analysis (elemental analysis data) where  $\text{Cl}^-$  or  $\text{SO}_4^{2-}$  ions are not precipitated colored by addition of  $\text{AgNO}_3$  or  $\text{BaCl}_2$  solutions, respectively, this tested good matched with CHN data.

All the complexes did not have electrolytic properties. This fact elucidated that the  $\text{Cl}^-$ ,  $\text{SO}_4^{2-}$  or  $\text{NO}_3^-$  are absent, and that the water molecules completely the coordination sphere of the orotate complexes.

### 3.3. Electronic absorption spectra

The spectra of the orotate complexes in DMF are shown in Fig. 3. There are two detected absorption bands at around (210, 235 nm) and 280 nm assigned to  $\pi-\pi^*$  and  $n-\pi^*$  transitions, respectively, in the electronic spectrum of the ligand. These transitions also found in the spectra of the complexes, but they are shifted towards lower wavelength, confirming the coordination of the ligand to the metallic ions. The first band around 210 and 235 nm is probably due to a  $\pi-\pi^*$  of the exocyclic band in heterocyclic ring and also assigned to the two carbonyl groups. However, the second band around 280 nm is due to presence of COOH group [34]. In case of  $[\text{UO}_2]^{2+}$ ,  $[\text{VO}]^{2+}$

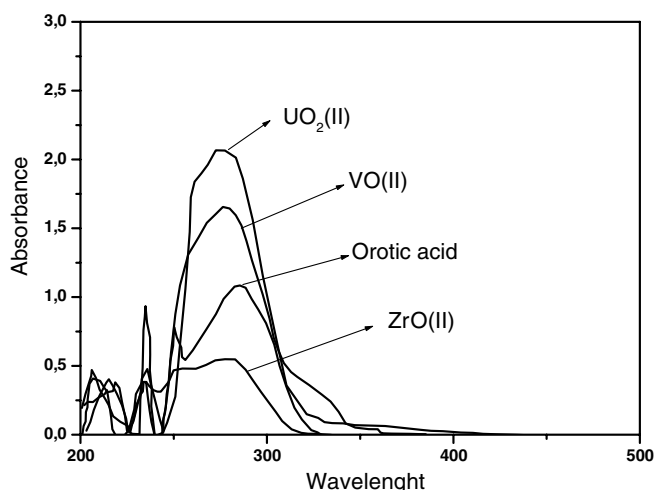


Fig. 3. Electronic spectra of orotic acid and their complexes.

and  $[\text{ZrO}]^{2+}$  orotate complexes, the carboxylic group is blue shifted with increase the intensity (absorbance). This result confirms the complexation of metal ions via carboxylic group (monodentate chelating). The  $[\text{VO}(\text{C}_5\text{H}_3\text{O}_4\text{N}_2)_2(\text{H}_2\text{O})_2] \cdot 6\text{H}_2\text{O}$  complex has a shoulder broad band at 325 nm may be assigned to the following d–d transition.

### 3.4. $^1\text{H}$ NMR spectra

The  $^1\text{H}$  NMR spectral data of the  $[\text{UO}_2(\text{C}_5\text{H}_3\text{O}_4\text{N}_2)_2(\text{H}_2\text{O})_2] \cdot \text{H}_2\text{O}$  complex and the free ligand ( $\text{H}_3\text{OA}$ ) orotic acid are collected in Table 3 and its spectrum is shown in Fig. 4. The literature values [35], of the  $^1\text{H}$  NMR chemical shifts ( $\delta$ , ppm) of orotic acid are included in Table 3 for comparison purposes. The presence of the N(1)–H and N(3)–H protons resonance in the spectrum (Table 3 and Fig. 4) clearly show that this nitrogen atoms not engaged in the complex formation. The uranyl(II) moiety appear to bind the orotic acid through carboxylate group, the absence of proton of (COOH) confirm the mode of coordination (behaves as a monodentate chelating ligand, binding through adjacent carboxylato group). The broad singlet peak at 4.45 ppm is due to the presence of water molecules protons and a multiplet signal around 6.57 ppm is due to the (C5)–H aromatic protons. Note that  $\text{H}_2\text{O}$  is seen in aprotic solvents, while HOD is seen in protic solvents due to exchange with the solvent deuteriums, this appeared in the spectrum of the  $[\text{UO}_2]^{2+}$  complex at 3.45 ppm.

It was found that orotic acid interacts with all of  $[\text{UO}_2]^{2+}$ ,  $[\text{VO}]^{2+}$  and  $[\text{ZrO}]^{2+}$  ions in the anionic form

and coordinates in a monodentate chelating through its carboxylate group. Vanadyl(II) and zirconyl(II) ions react with orotic acid in alkaline medium to form the four coordinated oxometal(IV) complexes of the type  $[\text{M}(\text{C}_5\text{H}_3\text{N}_2\text{O}_4)_2(\text{H}_2\text{O})_2](\text{H}_2\text{O})_n$ . The complexes are in the mononuclear form where the two orotate molecules and two water molecules occupy the four equatorial positions in a plan perpendicular to metal oxygen forming a square pyramid, and octahedral structure for  $[\text{UO}_2]^{2+}$  orotate complex see Scheme 1.

### 3.5. Mass spectra

The mass spectrum of orotic acid, ( $\text{H}_3\text{OA}$ ), ligand exhibits a prominent molecular ion at  $m/z$  (156, 64%). The fragmentation of orotic acid proceeds by loss of  $\text{CO}_2$  from the molecular ion to give uracil molecule at  $m/z$  113 with intensity 10%, then the elimination of  $\text{HNCO}$ , lead to the formation of an ion at  $m/z$  (68, 100%), which is the base peak of the spectrum. On the other hand, the probable loss of  $\text{CO}$  from the same ion (base peak, 68 (100%)) gives an ion at  $m/z$  40 (21%). The suggested pathway fragmentation pattern is given in Table 4 and Scheme 2.

The corresponding mass spectra of the uranyl(II), vanadyl(II) and zirconyl(II) orotate complexes are given in Table 4 and Fig. 5 and their fragmentation are presented in Schemes 3–5, respectively. Mass spectrometry has been applied in order to study the main fragmentation routes of some 6-carboxyuracil (vit B13) complexes. Difference in fragmentation was caused by the nature of the attached metal ions.

### 3.6. X-ray powder diffraction and scanning electron microscopy

X-ray powder diffraction patterns in the  $10^\circ < 2\theta < 70^\circ$  of the complexes were carried out in order to obtain an idea about the lattice dynamics of the complexes. By comparison of the obtained X-ray powder diffraction patterns shown in Fig. 6, the X-ray powder diffraction patterns throws light only on the fact that each solid represents a definite compound of a definite structure which is not contaminated with starting materials. This identification of the complexes was done by the known method [36]. Such facts suggest that the prepared compounds are amorphous.

Purity and morphology of the complexes obtained were studied by SEM. The obtained SEM micrographs, shown in Fig. 7, allow to verify that the  $[\text{UO}_2]^{2+}$ ,  $[\text{VO}]^{2+}$  and  $[\text{ZrO}]^{2+}$  complexes are the ones with the well formed amorphous shape. Such facts are in agreement with the obtained

Table 3

$^1\text{H}$  NMR data of orotic acid and uranyl(II) complex in  $\text{DMSO}-d_6$  solvent ( $\delta$ , ppm from TMS)

Compounds	Residual solvent	$^1\text{H}(\text{HDO})$	$\text{H}_2\text{O}$ coordination	N(1)–H	C(5)–H	N(3)–H	OH acid
$\text{H}_3\text{OA}$	–	–	–	6.00	6.74	10.00	11.00
$[\text{UO}_2]^{2+}$	2.51	3.45	4.45	6.42	6.57	8.96	–

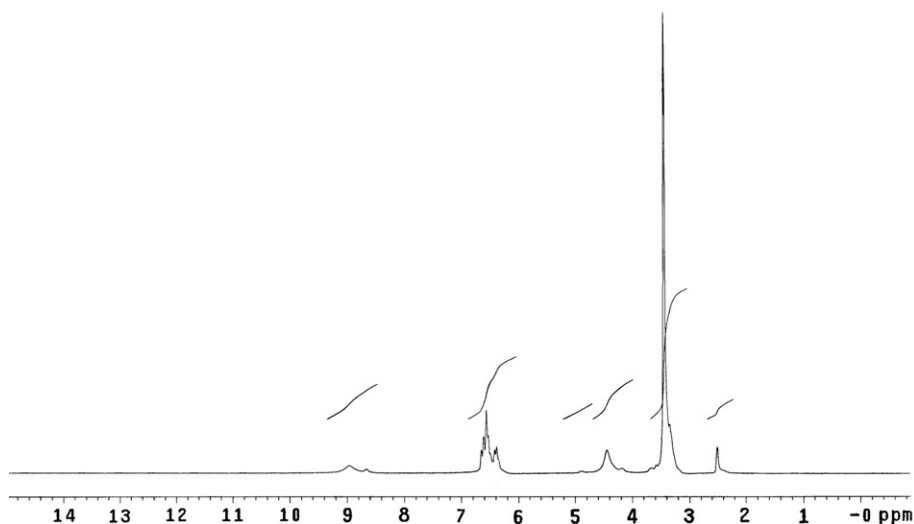
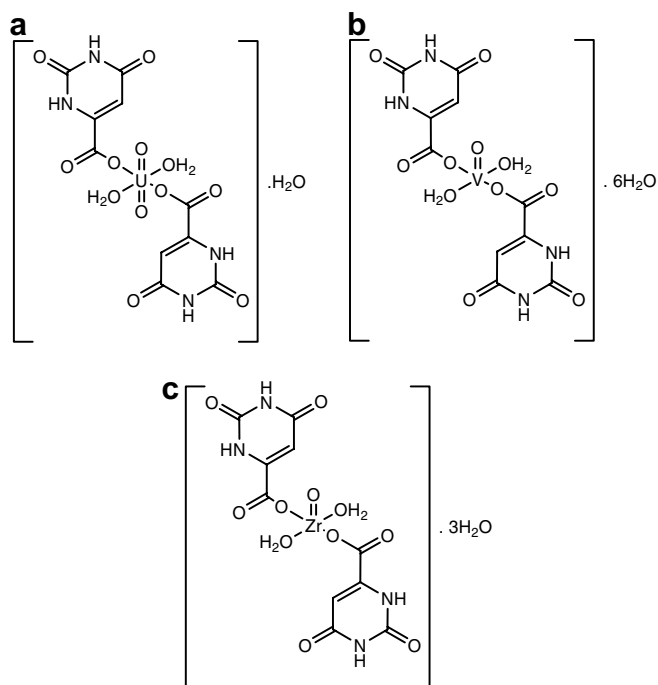


Fig. 4.  $^1\text{H}$  NMR spectra of uranyl(II) orotate complex.



Scheme 1. Suggested structure of (a) uranyl(II), (b) vanadyl(II) and (c) zirconyl(II)-orotate complexes.

X-ray results. Single crystals of the complexes could not be described. However, the spectroscopic data and elemental analysis of CHN supported to predict possible structures.

### 3.7. Thermogravimetric analysis

Thermal analysis curves (TG and DTG) of the studies complexes are shown in Fig. 8. The thermoanalytical results are summarized in Table 5.

#### 3.7.1. $[\text{UO}_2(\text{C}_5\text{H}_3\text{N}_2\text{O}_4)_2(\text{H}_2\text{O})_2] \cdot (\text{H}_2\text{O})$

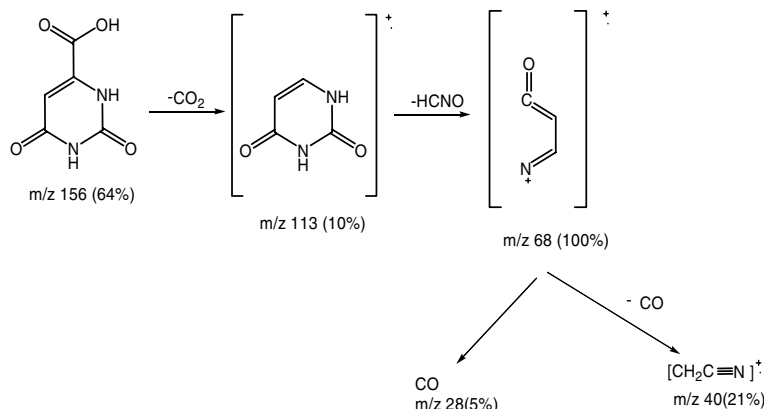
The thermal analysis curves of the complex show that decomposition takes places in three stages in 25–800 °C temperature range (Fig. 8). The first and second exothermic decomposition stages correspond to the dehydration process. The DTG and TG curves of the complex show a weight loss (Found 7.34, Calcd. 8.52%) in the 25–375 °C range corresponding to the loss of all three water molecules. The following stage is also exothermic at 432 °C (DTG) showing the decomposition of orotic acid. The final product, formed at *Ca.* 770 °C, consists of  $(\text{UO}_2 + 3\text{C})$ . Reported data on thermal analysis studies in the nitrogen atmosphere indicate that the  $[\text{UO}_2]^{2+}$  complex decompose to give oxide and few carbon atoms as final products, (no sufficiently of oxygen atoms help to evolved carbon as carbon monoxide or dioxide).

#### 3.7.2. $[\text{VO}(\text{C}_5\text{H}_3\text{N}_2\text{O}_4)_2(\text{H}_2\text{O})_2] \cdot 6(\text{H}_2\text{O})$

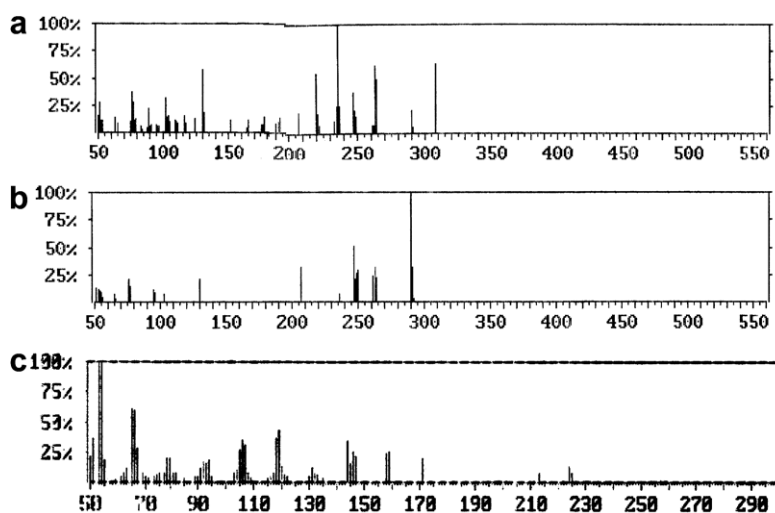
Thermal decomposition of  $[\text{VO}(\text{C}_5\text{H}_3\text{N}_2\text{O}_4)_2(\text{H}_2\text{O})_2] \cdot 6(\text{H}_2\text{O})$  proceeds in two ranged main stages. The first stage is related to the dehydration of crystalline water molecules (Found 20.20%; Calcd. 20.70%), in the temperature range, 25–408 °C, by giving an exothermic effect ( $\text{DTG}_{\text{max}}$ : 126,

Table 4  
Mass spectra data of  $[\text{UO}_2]^{2+}$ ,  $[\text{VO}]^{2+}$  and  $[\text{ZrO}]^{2+}$  complexes

Compounds	<i>m/z</i> (%)
Orotic acid ( $\text{C}_5\text{H}_4\text{O}_4\text{N}_2$ )	156(64); 113(10); 68(100); 40(21); 28(5)
$[\text{UO}_2(\text{C}_5\text{H}_3\text{N}_2\text{O}_4)_2(\text{H}_2\text{O})_2] \cdot (\text{H}_2\text{O})$	308(65); 290(21); 264(50); 247(37); 236(100); 220(56); 207(19); 130(58); 102(31); 76(37); 64(14); 51(28)
$[\text{VO}(\text{C}_5\text{H}_3\text{N}_2\text{O}_4)_2(\text{H}_2\text{O})_2] \cdot 6(\text{H}_2\text{O})$	290(100); 263(32); 247(51); 207(31); 130(21); 103(7); 76(20); 65(7); 51(12)
$[\text{ZrO}(\text{C}_5\text{H}_3\text{N}_2\text{O}_4)_2(\text{H}_2\text{O})_2] \cdot 3(\text{H}_2\text{O})$	224(3); 212(3); 171(5); 160(6); 152(5); 144(9); 131(11); 119(43); 106(34); 92(17); 78(19); 65(60); 54(100)



Scheme 2. Fragmentation pattern of orotic acid.

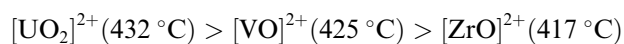
Fig. 5. Mass spectra of: (a),  $[\text{UO}_2]^{2+}$ ; (b),  $[\text{VO}]^{2+}$ ; and (c),  $[\text{ZrO}]^{2+}$  orotate complexes.

212 and 320 °C). In the following stage the anhydrous  $[\text{VO}]^{2+}$  complex decomposes in consecutive steps in the 408–750 °C temperature range to give  $\text{VO}_{2.5}$ .

### 3.7.3. $[\text{ZrO}(\text{C}_5\text{H}_3\text{N}_2\text{O}_4)_2(\text{H}_2\text{O})_2] \cdot 3(\text{H}_2\text{O})$

This complex decomposes in five stages (collected in two definite ranges). The first and second stages at (60 and 295 °C  $\text{DTG}_{\text{max}}$ , respectively) are exothermic decomposition and corresponding to the loss of three moles of uncoordinated water molecules (Found 10.20, Calcd. 10.70%). The anhydrous complex is stable up to 300 °C. The following stages involve the exothermic decomposition of the orotic acid ligands and coordinated water molecules, and then the final decomposition product is  $\text{ZrO}_2$ . The overall weight loss (Found 59.40, calcd. 59.60) agrees well with the proposed structure. The cause of higher temperature for liberated crystallized water molecules is due to the hydrogen bonding interaction with the coordination water molecules and orotate anions.

Based on the essential  $\text{DTG}_{\text{max}}$  temperatures of the decomposition of orotate complexes, the thermal stabilities of the complexes follow the sequence:



The proposed structures of the synthesized complexes which are presented in Scheme 1 are consistent with each other in term of chemical, spectroscopic data and thermal analysis.

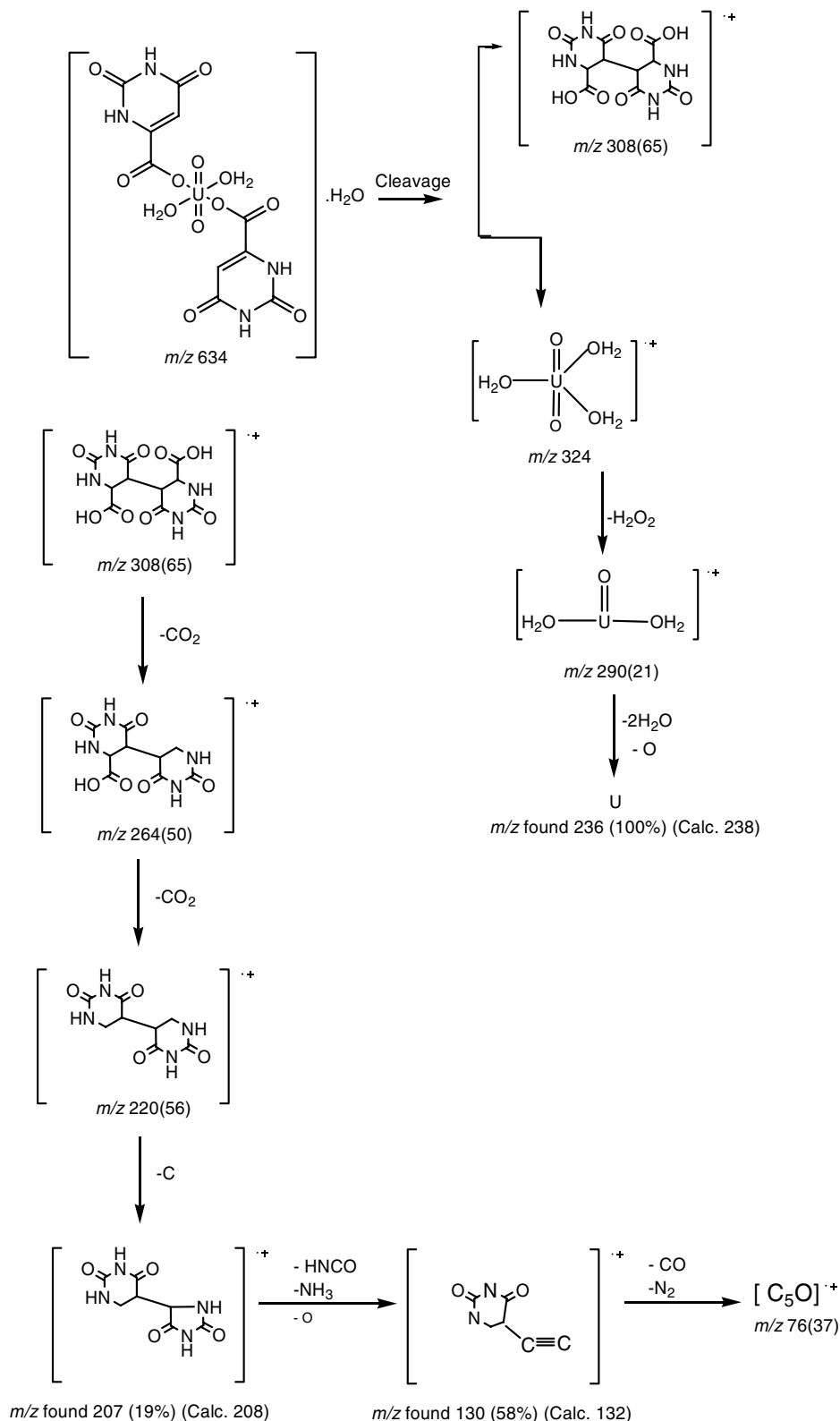
### 3.8. Kinetic parameters

Two methods are mentioned in the literature related to decomposition kinetics studies, Coats–Redfern [37] and Horowitz–Metzger [38], applied these two methods in this study.

### 3.9. Coats–Redfern equation

The Coats–Redfern equation (1), which is a typical integral method, can be represented as:

$$\int_0^\infty d\alpha / (1 - \alpha)^n = (A/\varphi) \int_{T_1}^{T_2} e^{-E^*/RT} dT \quad (1)$$

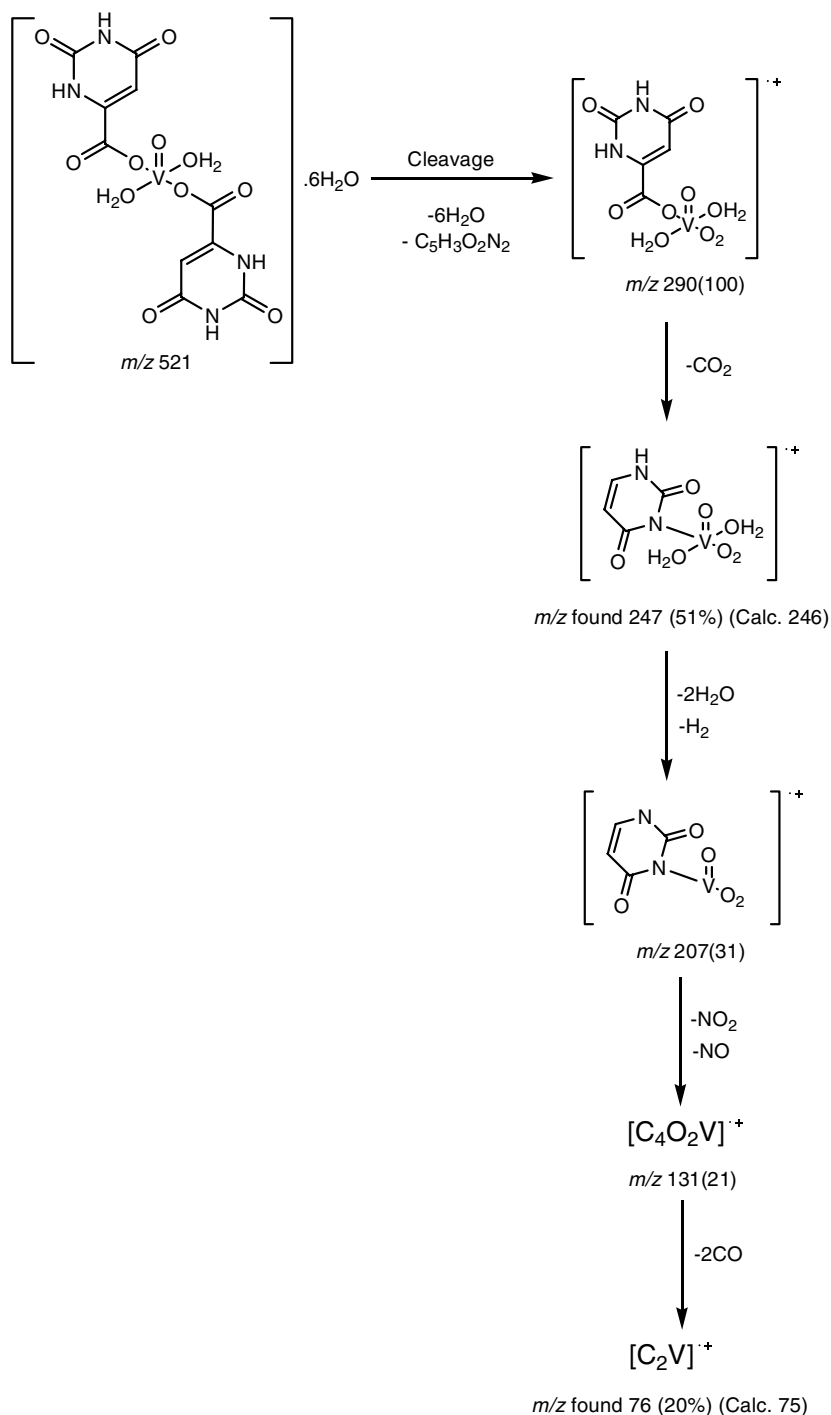


Scheme 3. Fragmentation pattern of uranyl(II) orotate complex.

For convenience of integration, the lower limit  $T_1$  is usually taken as zero. This equation on integration gives (Eq. (2));

$$\ln[-\ln(1 - \alpha)/T^2] = -E^*/RT + \ln[AR/\varphi E] \quad (2)$$

A plot of left-hand side (LHS) against  $1/T$  was drawn.  $E^*$  is the energy of activation in  $\text{KJ mol}^{-1}$  and calculated from the slop and  $A$  in  $(\text{s}^{-1})$  from the intercept. The entropy of activation  $\Delta S^*$  in  $(\text{JK}^{-1} \text{mol}^{-1})$  was calculated by using the equation:



Scheme 4. Fragmentation pattern of vanadyl(II) orotate complex.

$$\Delta S^* = R \ln(Ah/kT_s) \quad (3)$$

Where  $k$  is the Boltzmann constant,  $h$  is the Plank's constant and  $T_s$  is the DTG peak temperature.

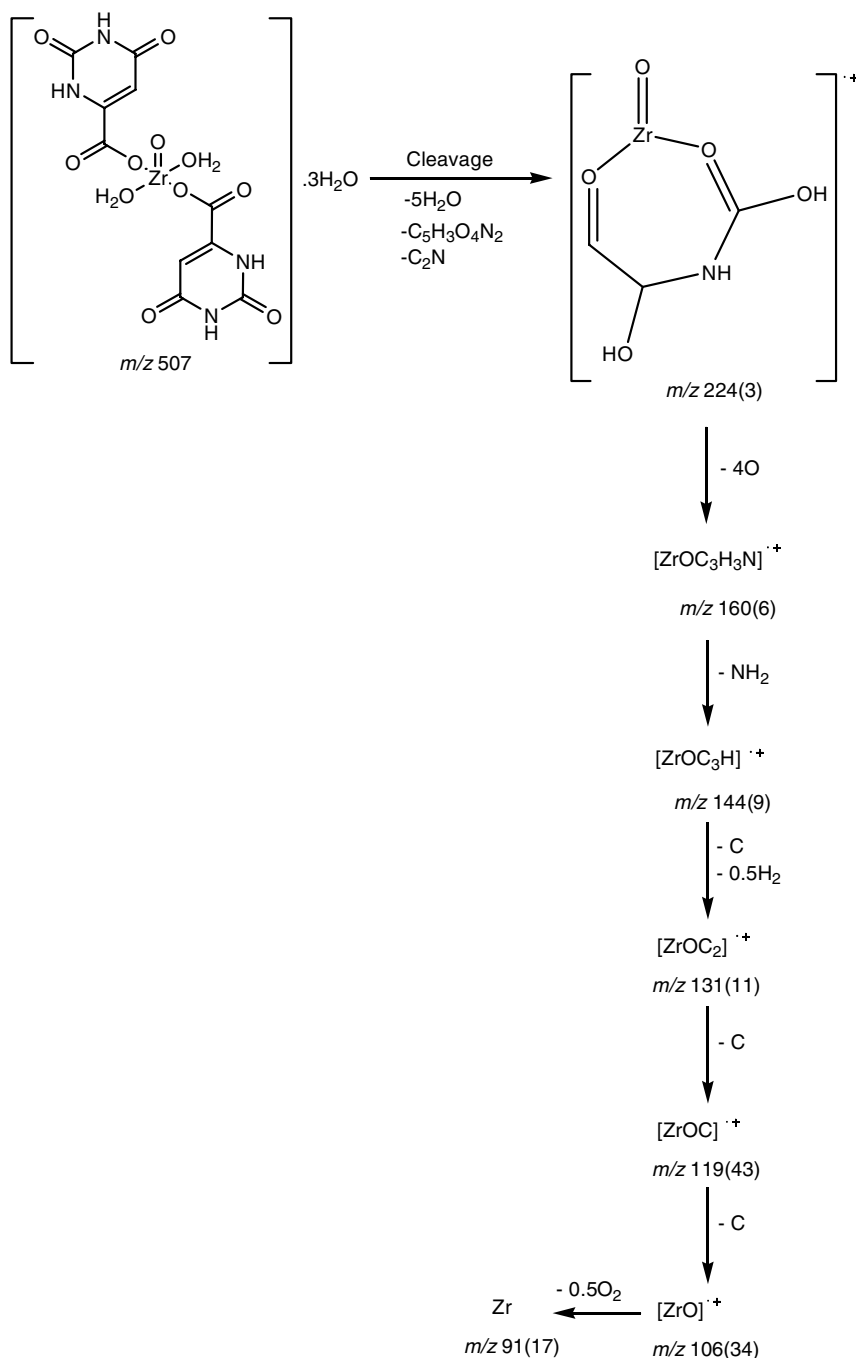
### 3.10. Horowitz–Metzger equation

The Horowitz–Metzger (Eq. (4)) was written in the form as follows:

$$\text{Log}[\log(w_x/w_\gamma)] = E^*\theta/2.303RT_s^2 - \log 2.303 \quad (4)$$

Where  $\theta = T - T_s$ ,  $w_\gamma = w_x - w$ ,  $w_x =$  mass loss at the completion of the reaction;  $w =$  mass loss up to time  $t$ . The plot of  $\text{Log}[\log(w_x/w_\gamma)]$  versus  $\theta$  was drawn and found to be linear from the slope  $E^*$  was calculated. The pre-exponential factor,  $A$ , was calculated from the Eq. (5):

$$E^*\theta/RT_s^2 = A/[\varphi \exp(-E^*/RT_s)] \quad (5)$$



Scheme 5. Fragmentation pattern of zirconyl(II) orotate complex.

The entropy of activation,  $\Delta S^*$ , enthalpy activation,  $\Delta H^*$ , and Gibbs free energy,  $\Delta G^*$ , were calculated from;

$$\Delta H^* = E^* - RT$$

$$\Delta G^* = \Delta H^* - T\Delta S^*$$

The linearization curves of Coats–Redfern and Horowitz–Metzger methods are shown in Fig. 9. Kinetic parameters for the main stages around 400 °C (decomposition of orotic acid), calculated by employing Coats–Redfern and Horowitz–Metzger equations, are summarized in

Table 6, together with the radii metal ions. The results show that the values obtained by various methods are comparable.

The kinetic data obtained with the two methods are in harmony with each other. The activation energy of  $[UO_2]^{2+}$ ,  $[VO]^{2+}$  and  $[ZrO]^{2+}$  complexes is expected increase in relation with decrease in their radius [39].

The  $E^*$  values calculated with the method of Coats–Redfern for the definite decomposition stages of the complexes are given below:

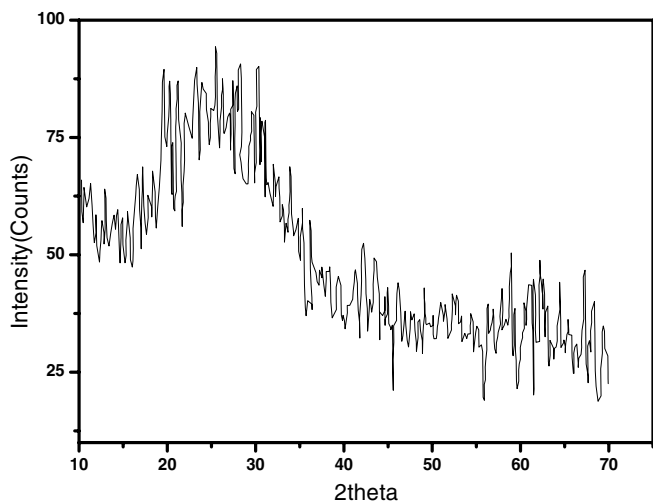


Fig. 6. X-ray diffraction patterns of uranyl(II) orotate complex.

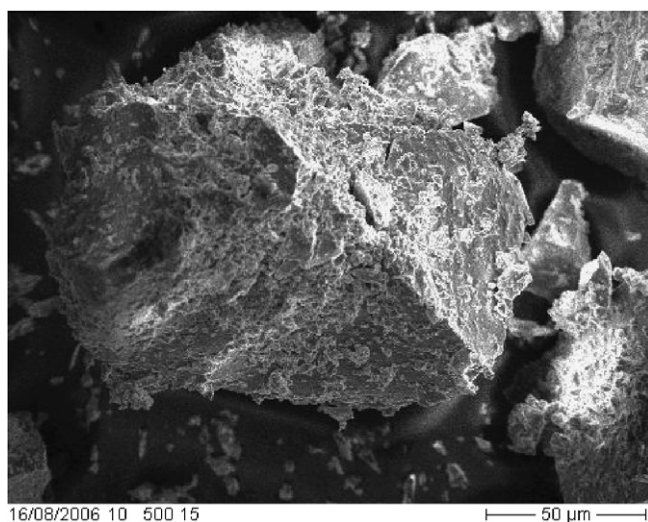


Fig. 7. SEM of uranyl(II) orotate complex.

$$E_{\text{UO}_2(\text{II})}^* = 227 \text{ kJmol}^{-1} > E_{\text{VO}(\text{II})}^* = 165 \text{ kJmol}^{-1} > E_{\text{ZrO}(\text{II})}^* = 127 \text{ kJmol}^{-1}$$

$$r_{\text{UO}_2(\text{II})} = 52 \text{ pm} < r_{\text{VO}(\text{II})} = 59 \text{ pm} < r_{\text{ZrO}(\text{II})} = 72 \text{ pm}.$$

### 3.11. Antibacterial activity

The preparation of stable metal orotate complexes is considerable important not only for their chemical but also biological and medical aspects. It is proven that orotic acid, formerly designated as vitamin B13, has a strong influence on regeneration geriatric cells, especially on the cells of the liver and the gastrointestinal tract. This may explain its important role in the geriatrics. Moreover, orotic acid is a carrier for a lot of minerals in the cells, which are partly of special important for the anticancer effects [40,41] with platinum and palladium(II) orotates.

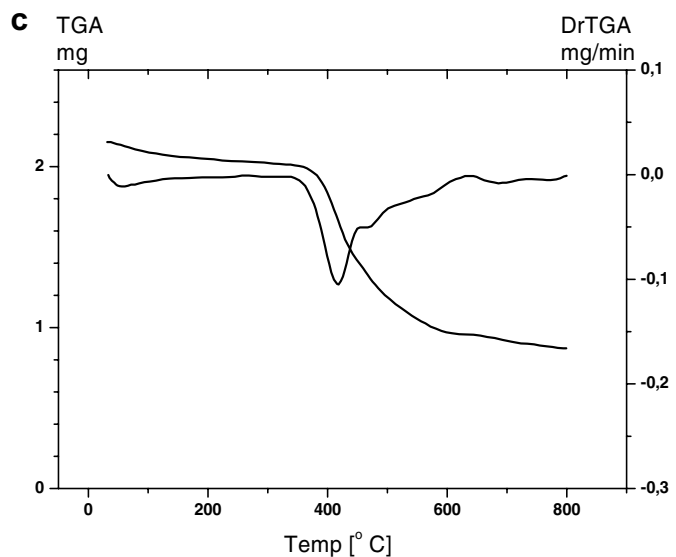
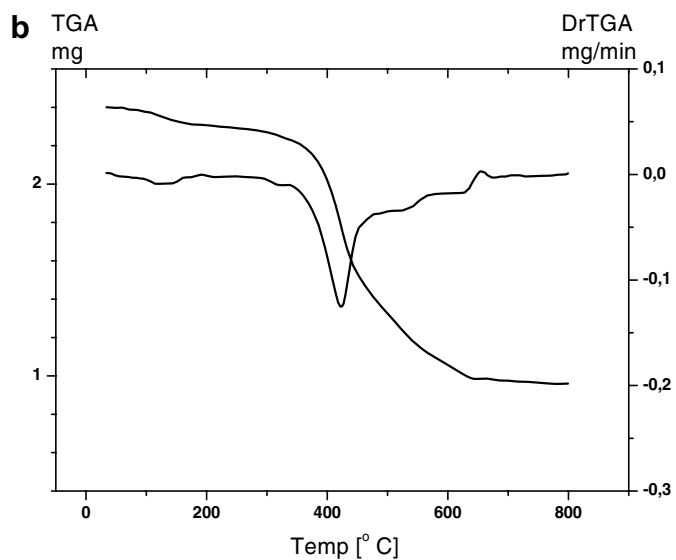
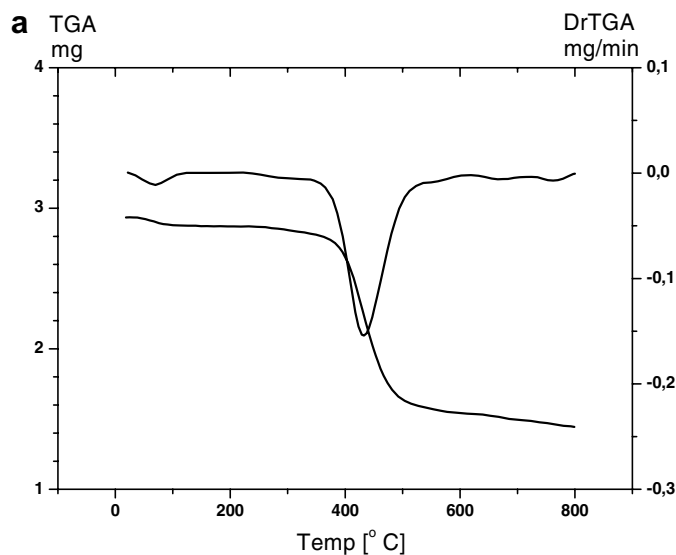
Fig. 8. Thermograms (TGA and DTG) of: (a),  $[\text{UO}_2]^{2+}$ ; (b),  $[\text{VO}]^{2+}$ ; and (c),  $[\text{ZrO}]^{2+}$  orotate complexes.

Table 5  
Thermoanalytical results (TG and DTGA) for isolated orotate complexes

Complexes	Stages	Temp./range (°C)	DTG <sub>max</sub> (°C)	Residual species	Decomposition species	Total losses (%)	
						Found	Calc.
[UO <sub>2</sub> ] <sup>2+</sup>	1St	25–215	68	UO <sub>2</sub> + 3C	–H <sub>2</sub> O cyst.	2.20	2.84
	2St	215–375	275		–2H <sub>2</sub> O coord.	5.14	5.68
	3St	375–800	432		7CO + NO + 2NH <sub>3</sub> + 0.5N <sub>2</sub>	43.60	43.20
[VO] <sup>2+</sup>	1St	25–408	126, 212, 320	VO <sub>2.5</sub> + 10C	–6H <sub>2</sub> O cyst.	20.20	20.70
	2St	408–800	425, 540, 655		4.5H <sub>2</sub> O + 4NO+ 0.5H <sub>2</sub>	39.40	38.80
[ZrO] <sup>2+</sup>	1St	25–390	60, 295	ZrO <sub>2</sub> + 7C	–3H <sub>2</sub> O cyst.	10.20	10.70
	2St	390–800	417, 471, 568		2H <sub>2</sub> O + 3CO+ 4NO + 3H <sub>2</sub> +	49.20	48.90

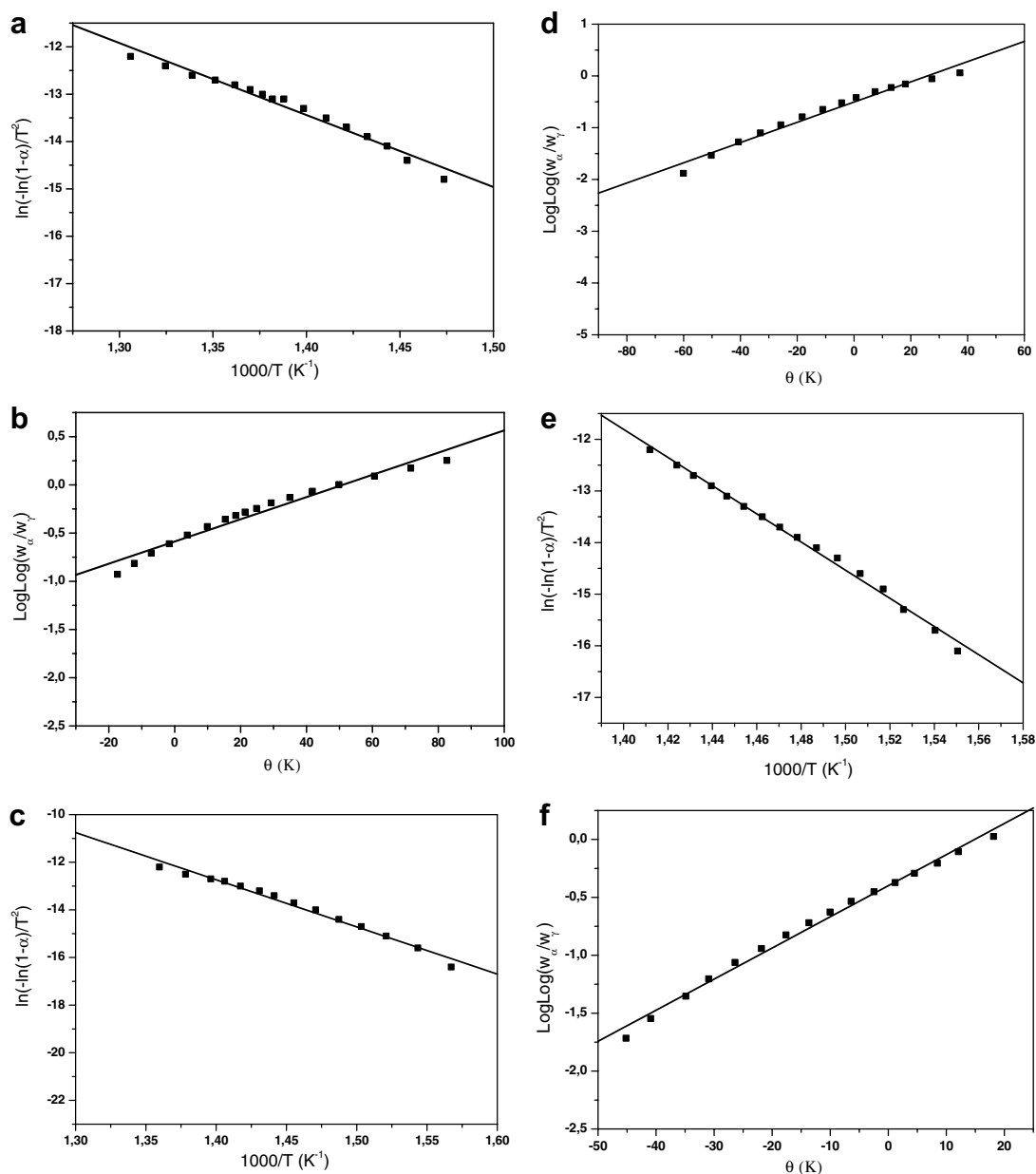


Fig. 9. The Diagrams of kinetic parameters of: (a), CR of [UO<sub>2</sub>]<sup>2+</sup>-orotate complex; (b), HM of [UO<sub>2</sub>]<sup>2+</sup>-orotate complex; (c), CR of [VO]<sup>2+</sup>-orotate complex; (d), HM of [VO]<sup>2+</sup>-orotate complex; (e), CR of [ZrO]<sup>2+</sup>-orotate complex; (f), HM of [ZrO]<sup>2+</sup>-orotate complex; Coats–Redfern, (CR); and Horowitz–Metzger, (HM) equations.

Table 6  
Thermal behavior and kinetic parameters determined using the Coats–Redfern (CR) and Horowitz–Metzger (HM)

Complexes	Radius metal ion/pm	T <sub>s</sub> (K)	Method	E* × 10 <sup>2</sup>	A	ΔS* × 10 <sup>2</sup>	ΔH* × 10 <sup>3</sup>	ΔG* × 10 <sup>4</sup>	r
[UO <sub>2</sub> ] <sup>2+</sup>	52	432	CR	2.27	1.99 × 10 <sup>12</sup>	−1.64	−5.51	5.83	0.9870
			HM	2.58	5.46 × 10 <sup>16</sup>	−1.73	−4.88	5.42	0.9812
[VO] <sup>2+</sup>	59	425	CR	1.65	1.60 × 10 <sup>7</sup>	−1.14	−5.64	7.40	0.9918
			HM	1.82	4.64 × 10 <sup>11</sup>	−1.23	−4.97	6.96	0.9876
[ZrO] <sup>2+</sup>	72	417	CR	1.27	1.99 × 10 <sup>12</sup>	−1.64	−5.51	5.83	0.9975
			HM	1.40	5.46 × 10 <sup>16</sup>	−1.51	−4.55	4.92	0.9961

Table 7  
Antibacterial activity of orotic acid and their complexes

Compounds	Gram positive		Gram negative	
	<i>Bacillus subtilis</i>	<i>Staphylococcus aureus</i>	<i>Escherichia Coli</i>	<i>Salmonella</i>
Orotic acid	++	+	++	++
[UO <sub>2</sub> ] <sup>2+</sup>	++++	+++	++++	+++
[VO] <sup>2+</sup>	++	–	+++	+
[ZrO] <sup>2+</sup>	+++	+++	++	+++

(–), NO antibacterial activity; (+), mild activity; (++) , moderate activity; (+++), marked activity; (++++), strong marked activity.

Applying the nutrient filter paper disc method all of the newly synthesized orotate complexes were screened *in vitro* for antibacterial activity against *E. Coli* and *Salmonella* (Gram negative bacteria) and *Bacillus subtilis* and *Staphylococcus aureus* (Gram positive bacteria). The activity was determined by measuring the diameter of the inhabitation zone. The screening results given in Table 7, indicated that all the complexes exhibited antibacterial activities against type of bacteria used.

An influence of the central ion of the complexes in the antibacterial activity against the tested Gram positive and Gram negative organisms. The results also show that the complexes have an enhanced activity compared to the orotic acid it self. This is specially showed against bacteria. The metal activity increase in the order



## References

- [1] G. Anastasi, M.L. Antonelli, A. Biondi, G. Vinci, *Talanta* 52 (2000) 947.
- [2] A. Hernanz, F. Billes, I. Bratu, R. Navarro, *Biopolymers* 57 (2000) 187.
- [3] I. Bratu, J.M. Gavira-Vallejo, A. Hernanz, M. Bogdan, Gh. Bora, *Biopolymers* 73 (2004) 451.
- [4] I. Bratu, J.M. Gavira, A. Hernanz, *Biopolymers* 77 (2005) 361.
- [5] I. Bratu, F. Veiga, C. Fernandes, A. Hernanz, J.M. Gavira, *Spectroscopy* 18 (3) (2004) 459.
- [6] J.J. Torres-Labandeira, J.L. Vila-Jato (Eds.), *Proc. of the Ninth Intern. Symp. On Cyclodextrins*, Kluwer Acad. Press, Dordrecht, 1999.
- [7] J. Leberman, A. Kornberg, E.S. Simms, *J. Biol. Chem.* 215 (1955) 403.
- [8] A. Lehninger, *Biochemistry*, Worth Publishers Inc., New York, 1970, pp. 661.
- [9] P. Arrizabalaga, P. Castan, F. Dahan, *Inorg. Chem.* 22 (1983) 2245.
- [10] O. Kumberger, J. Riede, H.Z. Schmidbaur, *Naturforsch.* 148 (1993) 961.
- [11] I. Bach, O. Kumberger, H. Schmidbaur, *Chem. Ber.* 123 (1990) 2267.
- [12] A. Psoda, Z. Kazimierczak, D. Shugar, *J. Am. Chem. Soc.* 96 (1974) 6832.
- [13] O. Bensaude, J. Aubard, M. Dreyfus, C. Dodin, J.E. Dubois, *J. Am. Chem. Soc.* 100 (1978) 2823.
- [14] B.E. Doody, E.R. Tucci, R. Scruggs, N.C. Li, *J. Inorg. Nucl. Chem.* 28 (1966) 833.
- [15] A.K. Singh, R.P. Singh, *Indian J. Chem.* 17A (1979) 469.
- [16] M. Sabat, D. Zglinska, B. Jeznowska-Trzebiatowska, *Acta Crystallogr.* B36 (1980) 1187.
- [17] A.Q. Wu, L.Z. Cai, G.H. Guo, F.K. Zheng, G.C. Guo, E.G. Mao, J.S. Huang, *Chin. J. Inorg. Chem.* 19 (2003) 879.
- [18] I. Mutakainen, R. Hamalainen, M. Klinga, O. Orama, U. Turpeinen, *Acta Crystallogr.* C52 (1996) 2480.
- [19] H. Icbudak, H. Olmez, O.Z. Yesilel, F. Arslan, P. Naumov, G. Javanowski, A.R. Ibrahim, A. Umsan, H.-K. Fun, S. Chant-rapronma, S.W. Ng, *J. Mol. Struct.* 657 (2003) 225.
- [20] A. Karipides, B. Thomas, *Acta Crystallogr.* C42 (1986) 1705.
- [21] I. Mutikainen, P. Lumme, *Acta Crystallogr.* B36 (1980) 2233.
- [22] T. Solin, K. Matsumoto, K. Fuwa, *Bull. Chem. Soc. Jap.* 54 (1981) 3731.
- [23] T.S. Khodashova, M.A. Porai-Koshits, N.K. Davidenko, N.N. Vlasova, *Koord. Khim.* 10 (1984) 262.
- [24] G. Maistralis, A. Koutsodimou, N. Katsaros, *Trans. Met. Chem.* 25 (2000) 166.
- [25] D.A. Köse, B. Zümreoglu-Karan, O. Şahin, O. Büyükgüngör, *J. Mol. Struct.* 789 (1–3) (2006) 147.
- [26] J.R. Lacher, J.L. Bitner, D.J. Emery, E.M. Seffl, J.D. Park, *J. Phys. Chem.* 59 (1955) 615.
- [27] T.S. Hermann, J.M. Black, *Appl. Spectr.* 20 (1966) 413.
- [28] E. Titov et al., *Khim. Heter. Soedin.* 6 (1972) 833.
- [29] L.S. Gelfand, F.J. Iaconianni, L.L. Pytlewski, A.N. Speca, C.M. Mikulski, N.M. Karayannis, *J. Inorg. Nucl. Chem.* 42 (1980) 377.
- [30] G.B. Deacon, R.J. Phillips, *Coord. Chem. Rev.* 33 (1980) 227.
- [31] S.P. McGlynn, J.K. Smith, W.C. Neely, *J. Chem. Phys.* 35 (1961) 105.
- [32] L.H. Jones, *Spectrochim. Acta* 15 (1959) 409.
- [33] J. Selbin, *Chem. Rev.* 65 (1965) 153.
- [34] G.D. Fasman, *Handbook of Biochemistry and Molecular Biology, Nucleic acids*, I, 65–215, CRC Pres.
- [35] S. Lencioni, A. Pellerito, T. Fiore, A.M. Giuliani, L. Pellerito, M.T. Cambria, C. Mansueto, *Appl. Orgomet. Chem.* 31 (1999) 145.
- [36] B.D. Cullity, *Elements of X-ray Diffraction*, Second ed., Addison-Wesley Inc., 1993.
- [37] A.W. Coats, J.P. Redfern, *Nature* 201 (1964) 68.
- [38] H.H. Horowitz, G. Metzger, *Anal. Chem.* 35 (1963) 1464.
- [39] N.K. Tunali, S. Ozkar, *Inorganic Chemistry*, Gazi University Publication, Pub. No. 185, Ankara, 1993.
- [40] P. Castan, E. Colacio-Rodriguez, A.L. Beauchamp, S. Cros, S. Wimmer, *J. Inorg. Biochem.* 38 (1990) 225.
- [41] A.D. Burrows, D.M.P. Mingos, A.J.P. White, D.J. Williams, *J. Chem. Soc. Dalton Trans.* 149 (1996).